（倫理面への配慮）

対象症例の両親に対し，研究主旨を説明し，調査報告することについて書面にて承諾を得，報告に関しては個人が特定されないように厳重な配慮を行った。

C．研究結果（表）

小児８例のうち新生児聴覚スクリーニング（NHS）の実施例は３例と少なく、うち１例は両耳ともにpass例であった。これにともない難聴の診断時期も２歳以上と遅い傾向が認められた。耳部CTおよびMRIにて前庭水管の拡大を評価し、両親の心情に応じて難聴遺伝子検査を案内し実施した。その結果全例でSLC26A4遺伝子が検出された。

成人４例は聴覚管理時、または聴力低下を訴えての再診時に、新たに画像診断を追加したものである。難聴遺伝子検査については１例（検索中）に承諾を得たのみであった。

なお、全例で聴力変動が認められ、変動時の低下状況に応じて外来あるいは入院にてステロイドの漸減療法を行った。この治療期間は、原則として補聴器は装用中止とした。

D．考案

対象の小児症例でNHS未実施例が多いことは、当院周辺地域でのNHS普及率を反映したものと考えられ、難聴診断が２歳以降という状況を生み出している。NHS実施例でも１例に両耳のpass児がみられており、NHSのみではなく、その後の観察と検診が重要であると再認識させられた。

前庭水管拡大を伴った感音難聴の場合、補聴器の効果が高く、人工内耳の適応も良好であることが報告されている。対象の小児例では補聴器装用の定着が早く、成人を含め全例で補聴効果は良好で、軽度知的障害を伴った１例を除いて言語発達は良好である。また、聴力変動の治療後に補聴器を再開した場合も、一時的な聴覚過敏などの反応はなく、受け入れが順調な印象があった。

聴力の変動については、本人および家族の動揺が著しく、変動が頻発することもあり、適切な投薬療法の検討と精神的な支援が不可欠であった。また補聴器の調整においては、聴力型が変化する場合もあり、症例によっては音量での対応とともにプログラムの切り替えなどを利用した方法が歓迎されている。聴力が著しく低下した場合は人工内耳が有効とはいえ、聴能活用の励行が必要であると思われた。

また成人症例については難聴遺伝子の検索を含めた原因精査が今後の課題と示唆された。

E．結論

前庭水管拡大を伴った感音難聴の12症例の臨床経過を検討した。聴覚障害の治療方法の確立はもとより、難聴の進行、めまい、甲状腺腫の合併などについてより確実な情報呈示が必要であると考えられた。

NO	年齢	性別	SLC26A4	NHS	難聴の診断	聴力		聴力型
						右	左	
1	2歳	F	K369E変異heterozygous H723R変異heterozygous	refer(両側)	5か月	77.5	63.8	高漸～水平
2	3歳	F	H723R変異heterozygous IVS10-2A>G変異heterozygous	未実施	2歳	82.5	72.5	水平
3	5歳	F	H723R変異homozygous	未実施	3歳	68.8	63.8	水平
4	7歳	M	stop at 556変異heterozygous IVS15+5G>A変異heterozygous	未実施	1歳半	81.3	92.5	高漸
5	7歳	M	H723R変異heterozygous IVS7-2A>G変異heterozygous	refer	6ヶ月	30.0	60.0	高漸～水平～低障
6	8歳	M	H723R変異homozygous	未実施	5歳	67.5	62.5	高漸
7	8歳	F	H723R変異heterozygous IVS7-2A>G変異heterozygous	両Pass	3歳	65.0	70.0	谷
8	13歳	F	H723R変異homozygous	未実施	7歳	48.8	31.3	左)低障　右)高急
9	19歳	F	未実施	未実施	3歳	77.5	82.5	高急
10	19歳	F	未実施	未実施	2歳	85.0	87.5	高漸
11	27歳	M	検索中	未実施	2歳	105.0	105.0	水平
12	38歳	M	未実施	未実施	2歳	90.0	103.8	水平

Ⅲ.　研究成果の刊行に関する一覧表

研究成果の刊行に関する一覧表レイアウト

書籍

著者氏名	論文タイトル名	書籍全体の編集者名	書　籍　名	出版社名	出版地	出版年	ページ
守本倫子	内耳疾患―染色体異常.	加我君孝	新生児・乳幼児の耳音響放射とABR	診断と治療社	東京	2012	112-117
		加我君孝	新生児・幼小児の耳音響放射とABR	診断と治療社	東京	2012	

雑誌

発表者氏名	論文タイトル名	発表誌名	巻号	ページ	出版年
Fujinami Y, Mutai H, Mizutari K, Nakagawa S, Matsunaga T	A novel animal model of hearing loss caused by acute endoplasmic reticulum stress in the cochlea.	J Pharmacol Sci	118	363-372	2012
Masuda S, Usui S, Matsunaga T	High prevalence of inner-ear and/or internal auditory canal malformations in children with unilateral sensorineural hearing loss.	Int J Pediatr Otorhinolaryngol	77	228-232	2013
Taiji H, Morimoto N, Matsunaga T	Unilateral cochlear nerve hypoplasia in children with mild to moderate hearing loss.	Acta Oto-Laryngologica	132	1160-1167	2012
守本　倫子	補聴器に関するQ&A－診療所における対応. Q33歳児検診にて発見された場合は？	ENTONI	144	19-22	2012
加我　君孝	中耳・内耳・中枢聴覚伝導路の発達	チャイルドヘルス	15(10)	696-700	2012

Ⅳ.　研究成果の刊行物・別刷

2. 内耳疾患(感音難聴)

5) 染色体異常

[国立成育医療研究センター感覚器・形態外科部耳鼻咽喉科] 守本倫子

染色体異常が認められる児は，幼少時は筋緊張の低下，口蓋裂などを伴っていることが多いため，滲出性中耳炎も伴いやすい．さらに先天性の中耳，内耳奇形に伴う感音難聴も認められる症例は少なくないが，聴力が改善または悪化してくる例もある．しかし精神発達遅滞があると音への反応がわかりにくく，さらに全身状態などが悪く，定期的な経過観察が困難な例もあるため，個々に対応していく必要がある．

┼ 病態生理

A 聴力変動

ダウン症候群をはじめとした染色体異常や神経疾患のなかには，生後6か月以内ではABR閾値が上昇していても2歳までに正常になることがあると報告されている[1]．その原因として，

①滲出性中耳炎が改善した可能性

②聴神経・脳幹の発達の未熟性

③反応の同期性の低下

があげられる．

新生児の中耳腔には間葉組織が残存しており，健常児では1歳まで，奇形・染色体異常では4～5歳までに吸収される．金らは，ABRにて閾値が改善した例ではほとんどの症例でⅠ波潜時の延長が認められ，蝸牛あるいは蝸牛神経の未熟性，または中耳の病変の両者が関与していることを指摘している[2]．中耳炎の治療のみで閾値改善する例や，当初高度難聴と診断されていた患者の聴力閾値が改善する症例もしばしば報告されており，難聴の診断の際は十分に念頭におくべきである．

B 21トリソミー(ダウン症候群)

1 難聴合併の疫学

ダウン症候群は21番染色体が3本あり，約800人に一人の割合で出生する．知的障害，心疾患，十二指腸閉鎖などの内臓奇形に加え，中耳炎や難聴を伴い，それが発達遅滞にさらに影響を及ぼすことがある．難聴は38～78％に一側または両側に認められ，70％は伝音難聴，20％は感音難聴，10％が混合性難聴とされている[3]．自験例では，ダウン症候群32症例中，感音難聴は6例(19％)伝音難聴13例(40％)混合性難聴9例(28％)であった．滲出性中耳炎にて鼓膜チューブ留置術を行ったのは20例(63％)であり，2例は慢性中耳炎であった．

2 原因

a) 滲出性中耳炎

ダウン症候群の児は，滲出性中耳炎を繰り返しやすい．この理由は，健常児に比べて咽頭が狭く，常に上気道感染と鼻汁が認められやすいこと，さらに筋緊張が弱く耳管機能が未熟であることがあげられる．飯野らは67例のダウン症候群児を検討し，全例両側または一側の滲出性中耳炎を合併していて，健常児よりもはるかに高率であったことが報告されている[4]．しかし，外耳道が細いうえ，診察に際して児の協力が得られにくいため，耳鏡で鼓膜所見をとりにくく滲出性中耳炎がはっきりわからないこともある．

b) 中耳奇形

幼少時に中耳炎に対して適切な治療を受けていなかったために，慢性中耳炎や中耳真珠腫を併発する例も少なくない．これにより慢性的な感染，耳漏により耳小骨の変形をきたし，伝音難聴が増悪する例もある．また，ダウン症候群児の側頭骨病理所見では，中耳腔に間葉性組織の残存とそれによる卵円窓，正円窓の閉鎖，耳小骨の異常なども報告されている．

c) 内耳奇形

全般において低形成であり，短蝸牛，半規管や前庭の奇形や蝸牛神経の低形成が有意に認められている．

d) 髄鞘化遅延

聴覚路は5歳まで髄鞘化が進むとされており，23％に髄鞘化不全があったとする報告もあれば，年齢相当である，という報告もある．

3 難聴の経過

a) 乳幼児期

ダウン症候群では外耳道が狭いことにより滲出性中耳炎などの鼓膜所見が十分にとれないこともあり，ABRのみで難聴が判断されてしまうことも少なくない．しかし，ダウン症候群の乳幼児におけるABRを検討した報告では，I波潜時延長が35％に認められたとされており，閾値上昇の原因は，①外耳道が細く，耳垢で閉塞しやすい，②滲出性中耳炎，③間葉系細胞残存による伝音難聴が多い．成長とともに外耳道も拡大し，滲出性中耳炎も軽快してきた例では閾値が改善し，さらに中耳伝音系に明らかな異常がなくても，2歳を過ぎた頃より高度難聴が改善してくる例では髄鞘化不全が原因として推測されている．

b) 成人後

早発老化現象として，思春期以降より徐々に聴力低下がみられることがある．

18～45歳の正常聴力のダウン症候群患者19例のABRを正常成人と比較したところ，III，V波潜時およびI－V波間潜時の短縮が認められており，この理由として，脳の容積が縮小していることと聴覚入力経路が単純化していることが考えられている[5]．

C Turner症候群

1 難聴合併の疫学

X染色体二つのうちの一つが欠損または一部欠損していることにより生じる．短頸で61％に反復性中耳炎の既往があり，鼓膜チューブ留置も32～57％に必要であったとされている．難聴合併頻度は約50％とされているが，感音難聴は思春期を過ぎた頃から，特に谷型～高音域を中心に低下してきて，核型が完全欠損型(45，XO)では早期から進行するのに対し，モザイク型

ではやや緩徐に進行する傾向がある[6].

2 原因

a) **伝音難聴**

頸部リンパ浮腫や高口蓋に伴う耳管の解剖学的異常により，反復性中耳炎，滲出性中耳炎になりやすく軽度伝音難聴を呈しやすい．また，十分に治療が行われていなかった場合，慢性中耳炎や真珠腫にもなりやすいため，中等度難聴を呈することもある．中耳疾患の既往は完全欠損型で80％に認められたものの，モザイク型では50％程度であった．

b) **感音難聴**

①**エストロゲン分泌不全**：内耳のコルチ器にはエストロゲンの受容体が分布しており，思春期から分泌が亢進するエストロゲンが十分に分泌されないことにより内耳が変性してくるという説はあるが，血中エストロゲン濃度と難聴について明確な相関が認められていない．

②IGF-1 **分泌不全**：最終身長と難聴の程度が比例していることから，幼少時に成長ホルモンが十分に分泌されなかったことにより聴力低下をまねくという説がある．しかし，成長ホルモン投与を行っても感音難聴には効果がなかったと報告されている．

③**遺伝子欠損**：細胞の新陳代謝と成長をつかさどるとされているSHOX(short stature homeobox-containing)遺伝子がX染色体のP腕にあり，これが欠損している完全欠損型(XO)では聴力の進行が著しいという説で，最も有力と考えられている[7].

3 難聴の経過

思春期を過ぎた頃から高音域の聴力が低下するため，社会に出た頃より難聴を自覚することも少なくない．20歳以上では2年ごとに定期的な聴力の評価を行い，必要に応じて補聴器装用が必要となる．

D その他の染色体異常

1 難聴合併の疫学

佐野は，染色体異常があって聴力検査を行ったもののうち，51名(32.9％)に難聴が認められたと報告しており[8]，常染色体異常では21トリソミー以外の28例では64％に難聴が認められたとされている．また，Velocardial症候群(22q 11.2欠失症候群)などは統計がほとんどないが，難聴合併率が65％(感音性19％，混合性28％，伝音性17％)とされており，特に高周波数域に閾値上昇を認めるとされている[9].

2 原因

a) **中耳疾患**

Velocardial facial症候群では，口蓋裂や粘膜下口蓋裂を伴っているため，耳管機能不全があり滲出性中耳炎を伴いやすく，軽度以上の伝音難聴を呈する．

b) **内耳奇形**

13トリソミーでは，蝸牛および半規管の形成不全と，顔面神経の走行異常および前庭神経，蝸牛神経の低形成が，18トリソミーでは外耳および中耳の低形成，間葉成分の残存と，蝸牛形成不全や欠損などが報告されており，発生段階での高度の形成不全が原因となっている．

検査法とその組み合わせ

A 乳幼児聴力検査(BOA, COR, peep show test)

染色体異常がある児では，知的発達の遅れも認められるため，十分に聞こえる音を呈示しても全く興味を示さないことが多い．このため，難聴が発見しにくく，注意深い観察や検査が必要となる．しかし，ABR で無反応であってもかなり小さな音に反応が認められる場合もあり，低周波数領域の音が聞こえている可能性や髄鞘化不全または同期不全の可能性もある．また，当初 COR(conditioned orientation response audiometry：条件詮索反応聴力検査)の音刺激に反応がなかったものが，徐々に反応するようになり，ABR を行ったところ，閾値改善している例もよく経験する．音刺激による条件づけを行ってボタンなどを押す peep show test は相当成長発達し，練習しないと困難であることが多い．

B OAE(耳音響放射)検査

染色体異常がある児は，滲出性中耳炎の合併率も高く，外耳道が狭いこともあるため多くの例で反応が不良となることが多い．また，髄鞘化不全など中枢神経系の異常や蝸牛神経の形成不全では，OAE 検査では良好な反応が得られることもあるため，補助的な診断方法として行うべきである．

C ABR, ASSR

I 波の潜時延長がある場合は，滲出性中耳炎や中耳奇形などの中耳疾患や蝸牛神経低形成などを念頭におくべきであり，側頭骨 CT などの画像検索を検討する．ASSR(auditory steady-state response：聴性定常反応)は周波数ごとの聴力閾値が測定可能であるため，染色体異常で COR での反応が明確ではない児に対して有用である．また，補聴器を装用して音場検査で閾値を測定することもできる．

症例呈示

A 患者プロフィールと検査

年齢・性別	9 歳，女児　9p- 症候群 West 症候群
検査法	新生児スクリーニング(DPOAE，ABR)で難聴を指摘，ティンパノグラムにて滲出性中耳炎を診断後，両側鼓膜チューブ留置後 ABR にて高度感音難聴の診断を行った．口蓋裂あり．側頭骨 CT では異常なかったため COR にて経過観察していたところ，4 歳で ABR 正常化した．
検査のコツ	染色体異常の児に対しては，まず滲出性中耳炎による影響を排除してから検査を行う．側頭骨 CT による情報は有用である．

B 検査所見

1 初診時(生後 6 か月)

初診時(生後 6 か月)の ABR では 70 dB と閾値上昇を認めたが，同時に I 波潜時の延長が認め

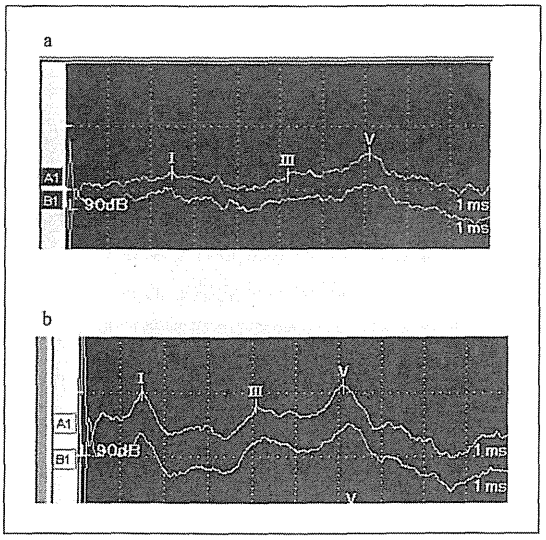

図1 症例のABR波形
a. 6か月時
I波潜時の延長があり，聴力閾値は70 dBであった．
b. 9か月時
鼓膜チューブ留置後，I波潜時は正常児と同じ程度に短縮した．

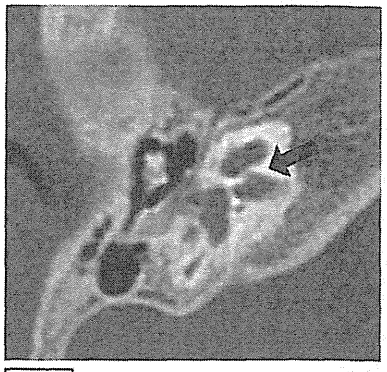

図2 蝸牛神経狭窄例
中等度難聴を呈するダウン症男児の側頭骨CT
染色体異常では，内耳奇形が多くみられるため，予後予測にも有用である．

られ，耳鏡所見，ティンパノグラム両側B型であったことから両側滲出性中耳炎と診断した(**図1a**)．CORでは100 dBにてようやく反応が認められた．

2 鼓膜チューブ留置術後

両側滲出性中耳炎に対して，両側鼓膜チューブ留置術施行．術後のABRを**図1b**に示す．I波潜時が明らかに短縮しているのがわかる．このときのABRでの聴力閾値は60 dBと改善した．側頭骨CTでは明らかな異常なし．CORでも80 dBにて反応がみられるようになった．

3 4歳時

CORでは明らかな変化は認められなかったが，家庭での声かけに反応が良好になってきたとのことで再度ABR施行．閾値は40 dBまで低下した．定期的にCORにて経過をみたところ，9歳時では40 dBで良好な反応を示すことができた．

C 鑑別診断のポイント

染色体異常の児は脳幹発達が未熟であるため，1歳未満でABRの閾値が上昇していた場合，改善する可能性も期待できる．しかしあくまでも「改善の可能性」であって，確証ではない．しかし反対に内耳奇形の合併率も高いため，側頭骨CT(**図2**)やMRIにより確認し，改善する見込みがあるかないかを予測することも重要である．

見逃しやすいポイント

・発達遅滞がある児の聴力検査は，何度か繰り返して行わないと正確な反応はわかりづらい．正常乳幼児でもCORにて40 dB程度の音に確実に反応がみられるのは生後8か月ごろからである．このため，CORで反応が乏しかった場合に難聴を疑うか，音刺激への反応が乏しいだけとみなすか，しっかり判断することが必要である．

・染色体異常の児のABRでは波形の不分離や潜時の延長などが生じやすい．その原因として脳幹発達が未熟であるためか，滲出性中耳炎によるものか，耳鏡所見，ティンパノグラム，側頭骨CT，MRIなどを用いて診断し，中耳炎の治療や補聴器装用など，適切な治療を行うことが大切である．

文献

1) 加我君孝：聴覚の発達の基礎．加我君孝(編)：新生児聴覚スクリーニング—早期発見・早期療育のすべて．金原出版，2005；99-106
2) 金　玉蓮，新正由紀子，加我君孝ほか：Otol Jpn 2006；16：171-177
3) Northern JL, Downs MP：Hearing in children. 5th ed, Lippincott, 2002；95-96
4) 飯野ゆき子：耳鼻臨床 1996；89：929-936
5) Forti S, Amadeo Ç, et al.：Brain Res 2008；1233：58-62
6) Morimoto N, Tanaka T, et al.：J Pediatr 2006；149：697-701
7) Barrenäs M, Landin-Wilhelmsen K, et al.：Hear Res 2000；144：21-28
8) 佐野光仁：JOHNS 2000；16：1705-1707
9) Zarchi O, Attias J, et al.：J Pediatr 2011；301-306

J Pharmacol Sci 118, 363 – 372 (2012)

Journal of Pharmacological Sciences

Full Paper

A Novel Animal Model of Hearing Loss Caused by Acute Endoplasmic Reticulum Stress in the Cochlea

Yoshiaki Fujinami[1,#,†], Hideki Mutai[1,†], Kunio Mizutari[1], Susumu Nakagawa[1], and Tatsuo Matsunaga[1,*]

[1]*Laboratory of Auditory Disorders, National Institute of Sensory Organs (NISO), National Tokyo Medical Center, 2-5-1 Higashigaoka, Meguro-ku, Tokyo 152-8902, Japan*

Received December 2, 2011; Accepted January 12, 2012

Abstract. Many stimuli such as ischemia, hypoxia, heat shock, amino acid starvation, and gene mutation, exhibit a cellular response called endoplasmic reticulum (ER) stress. ER stress induces expression of a series of genes, leading to cell survival or apoptosis. Previously, we found that in an animal model of hearing loss caused by acute mitochondrial dysfunction, several ER stress markers including C/EBP homologous protein were induced in the cochlear lateral wall. To elucidate the mechanism of hearing loss caused by ER stress, we established a novel animal model of hearing loss by perilymphatic perfusion of tunicamycin, an ER stress activator that inhibits *N*-acetylglucosamine transferases. Subacute and progressive hearing loss was observed at all sound frequencies studied, and stimulation of ER stress marker genes was noted in the cochlea. The outer hair cells were the most sensitive to ER stress in the cochlea. Electron microscopic analysis demonstrated degeneration of the subcellular organelles of the inner hair cells and nerve endings of the spiral ganglion cells. This newly established animal model of hearing loss from ER stress will provide additional insight into the mechanism of sensorineural hearing loss.

Keywords: endoplasmic reticulum stress, tunicamycin, hearing loss, animal model

Introduction

Hearing loss is a major communicative disorder that influences personal and social activities of afflicted patients. Although developments in medicine and engineering have significantly improved adaptive strategies for patients with hearing loss, many types of sensorineural hearing loss, such as sudden deafness and Meniere's disease, still require effective therapeutic strategies. One of the difficulties in developing effective therapeutic methods for such patients is the lack of knowledge about the molecular and cellular events causing the hearing disorders. To elucidate the mechanism underlying acute hearing loss due to cochlear energy failure such as what occurs in cochlear ischemia, we previously established an animal model of acute hearing loss using the mitochondrial toxin 3-nitropropionic acid (3-NP) (1, 2). In this model, expression of endoplasmic reticulum (ER) stress marker genes such as C/EBP homologous protein (*chop*, also called *Ddit3* or *Gadd153*) and activating transcription factor 4 (*Atf4*, also called *Creb2*) was upregulated in the cochlear lateral wall (LW) when primary injuries were detected (3), suggesting that ER stress plays a role during the onset or exacerbation of hearing loss in some types of auditory disorders.

A number of reports have indicated that ER stress in various organs is related to conditions such as Alzheimer's disease (4), Parkinson's disease (5), ischemia-reperfusion injury (6), diabetes (7), and cystic fibrosis (8). Tunicamycin, an inhibitor of *N*-acetylglucosamine transferases, has been widely used to examine ER stress and subsequent molecular and cellular events (9). Tunicamycin inhibits the first step of *N*-linked glycosylation of immature proteins (10) and ultimately causes apoptosis in vitro (11). Blockage of *N*-linked glycosylation results in the accumulation of misfolded and/or misassembled proteins in the ER, which typically stimulates the so-called ER stress marker genes, including *chop*, *Atf4*, glucose-regulated protein 78 (*grp78*, also called *Bip* or *Hspa5*), and *grp94* (also called *Hsp90β1* or *Tra1*) (12). In vivo injec-

#Dr. Yoshiaki Fujinami passed away in February 2012.
†These authors equally contributed to this work.
*Corresponding author. matsunagatatsuo@kankakuki.go.jp
Published online in J-STAGE on February 23, 2012 (in advance)
doi: 10.1254/jphs.11227FP

tion of tunicamycin causes death of retinal ganglion cells (13, 14). No studies on the cellular and molecular mechanisms of tunicamycin for ER stress in the inner ear have been performed.

In this study, we established a novel animal model of ER stress–induced hearing loss by perilymphatic perfusion of tunicamycin into the rat inner ear and elucidated the pathological mechanism at the physiological, morphological, and molecular levels to reveal unique features of cochlear responses to ER stress.

Materials and Methods

Animals and drug administration

Male 6- to 8-week-old Sprague-Dawley rats (weighing 170 – 230 g; Charles River Lab. Japan, Yokohama) were used to establish the hearing loss model. They were housed in metallic breeding cages in a room with a 12-h light/dark cycle, 55% humidity, and at 23°C, and the rats were permitted free access to food and water for at least 7 days before use.

The rats were anesthetized by inhalation of 1.5% – 3.0% isoflurane (2.0 L/min air flow) delivered via a mask using an anesthetizer (model TK-5; Muromachi Kikai, Tokyo), together with local anesthesia by injection of 1% lidocaine. The surfaces of the posterior and lateral semicircular canals of the left inner ear were exposed, and a small hole was made in each canal. A small tube (Eicom, Kyoto) was inserted into the lateral semicircular canal toward the ampulla. Through this tube, the perilymph was perfused with tunicamycin (Wako Pure Chemical, Osaka) for 8 min at a rate of 5 μL/min using a syringe pump. Drainage was allowed through a hole on the posterior semicircular canal. The tube was then removed, the holes on the semicircular canals were sealed with a piece of muscle and fibrin adhesive (Beriplast P Combi-set; CSL Behring, King of Prussia, PA, USA), and the wound on the neck was closed. Tunicamycin was dissolved at 0.5 to 500 ng/μL in saline containing PURE BRIGHT MB-37-50T (NOF Corp., Tokyo), which enhances drug solubility (15). An equal volume of vehicle without tunicamycin was injected into the semicircular canal of another group of animals as a control. The cochlea on the contralateral side (right side) was surgically destroyed to avoid cross hearing during ABR measurement. All experimental procedures were approved by the Institutional Animal Care and Use Committee of National Tokyo Medical Center.

Measurement of auditory brainstem response (ABR)

ABR thresholds were recorded from rats before surgery and at 1, 2, 3, and 7 days after treatment (DAT) with serial doses of tunicamycin (n = 3 in each group) or vehicle (n = 4), and additional 14, 21, and 28 DAT with 5 ng/μL of tunicamycin, vehicle, or untreated (n = 3) using Scope wave form storing and stimulus control software and the PowerLab data acquisition and analysis system (PowerLab2/20; AD Instruments, Castle Hill, Australia). Pure tone bursts of 8, 20, and 40 kHz (0.2 ms rise/fall time, 1 ms flat segment) and the amplitudes were specified by a real-time processor and programmable attenuator (RP2.1 and PA5; Tucker-Davis Technologies, Alachua, FL, USA). Sound levels were calibrated using a sound level meter (NL32; RION, Tokyo). Waveforms of 512 stimuli at each frequency were averaged and the visual detection threshold was determined with increment or decrement of sound pressure level by 5-dB steps. Details of ABR recording have been described previously (1). The thresholds were evaluated as the means ± S.E.M., and statistical significance was determined with two-way ANOVA.

Light microscopy and fluorescent microscopy

For morphological analysis with light microscopy using tissue sections, rats ($n \geq 3$ for each period in a series of experiments) were deeply anesthetized with pentobarbital (50 mg/kg, i.p.) and perfused intracardially with 0.01 M phosphate–buffered saline (PBS, pH 7.4) containing 8.6% sucrose, followed by 4% paraformaldehyde (PFA) in PBS. After decapitation, temporal bones were removed quickly and placed in the same fixative. Small openings were made at the round window, oval window, and apex of the cochlea. After immersion in the fixative overnight, the temporal bones were decalcified in 5% EDTA and 4% sucrose in PBS at 4°C for 2 weeks, dehydrated, and embedded in paraffin. Transverse cochlear sections (5-μm-thick) were cut and mounted on glass slides. After rehydration, sections were stained with hematoxylin and eosin. To analyze hair cells using surface preparation of cochleae, the cochleae from rats treated with vehicle or 5 ng/μL tunicamycin at 7 DAT were immediately fixed with 4% PFA in PBS overnight at 4°C and then decalcified in 5% EDTA and 4% sucrose in PBS at 4°C for 3 days. Following decalcification, the optic capsules were removed, and the samples were treated with 0.3% Triton-100 in PBS for 5 min. The samples were stained with rhodamine-phalloidin (70 nM in PBS) for 60 min at room temperature (16). Then, the organ of Corti was separated from the lateral wall and modiolus, microdissected into individual turns, counterstained with DAPI (1 μg/mL; DOJINDO, Kumamoto), and mounted on glass sides in PermaFluor Aqueous Mounting Medium (Thermo Fisher Scientific, Waltham, MA, USA).

Quantitative reverse transcription PCR (qRT-PCR)

After the rats were anesthetized, temporal bones were quickly removed, and immersed in RNAlater (TaKaRa Bio, Shiga) on ice, followed by dissection of whole cochleae. Total RNA was isolated with TRIzol Reagent (Life Technologies, Carlsbad, CA, USA) and dissolved in DEPC-treated water, and the purity of total RNA was determined by the ratio of OD_{260}/OD_{280} as measured on a UV/visible spectrophotometer (Ultrospec 2100 pro; GE Healthcare, Uppsala, Sweden). First-strand cDNA synthesis was performed using 100 ng of total RNA and Oligo $(dT)_{12-18}$ primers (Life Technologies) in a total volume of 20 μL according to the SuperScript III RNase H^- Reverse Transcriptase protocol (Life Technologies). qRT-PCR was performed according to the manufacturer's protocols for the ABI PRISM 7000 Sequence Detection System (Life Technologies). We designed PCR primers specific for *chop*, *Atf4*, *grp78*, *grp94*, and glyceraldehyde-3-phosphate dehydrogenase (*gapdh*). The specificity of these primer sets has been previously confirmed (3). qRT-PCR was performed in a 25-μL reaction containing 1 × SYBR Premix Ex Taq (TaKaRa Bio), 1 × ROX Reference Dye, 0.2 μM of each primer, and cDNA. The PCR conditions were 5 s at 95°C and 31 s at 60°C for 40 cycles. Gene expression levels were normalized using *gapdh* as an internal control. Statistical significance was evaluated using Student's *t*-tests adjusted with Holm's procedure.

Electron microscopy

Rats were deeply anesthetized by intraperitoneal injection of pentobarbital (50 mg/kg) and perfused intracardially with Lactec buffer (Otsuka Pharmaceutical, Tokyo), followed by perfusion-fixation with 4% PFA and 4% glutaraldehyde in 30 mM HEPES buffer (pH 7.4). After decapitation, temporal bones were removed quickly and placed in the same fixative. Small openings were made at the round window, oval window, and apex of the cochlea. After immersion in the fixative overnight, the temporal bones were decalcified in 4% EDTA and 5% sucrose in PBS at 4°C for 5 days. After washing in 60 mM HEPES buffer, the tissue was postfixed in 1% OsO_4 in 30 mM HEPES buffer for 4 h at 4°C, dehydrated in a graded ethanol series and QY-1 (Nisshin EM, Tokyo), and embedded in Epon resin. Ultra-thin sections in the horizontal plane parallel to the cochlear modiolus were cut with a MT2-B ultra micro-tome (Sorvall, Newtown, CT, USA) and mounted on 100-mesh grids. The sections were stained with uranyl acetate and lead citrate and were examined with a H600 electron microscope (Hitachi, Tokyo).

Results

ABR threshold shifts after ER stress and distinct vulnerability to ER stress among different cell types in the cochlea

We first examined changes in the hearing level after exposure to various degrees of acute ER stress by measuring ABR in rats up to 7 DAT with tunicamycin (Fig. 1: A – D). Then, we examined the differences in vulnerability to ER stress among different cell types in the cochlea by morphological analysis.

Rats treated with 0.5 ng/μL tunicamycin demonstrated a moderate increase in the ABR threshold from below 25 dB before treatment to 51.0 ± 14.1 dB at 40 kHz at 1

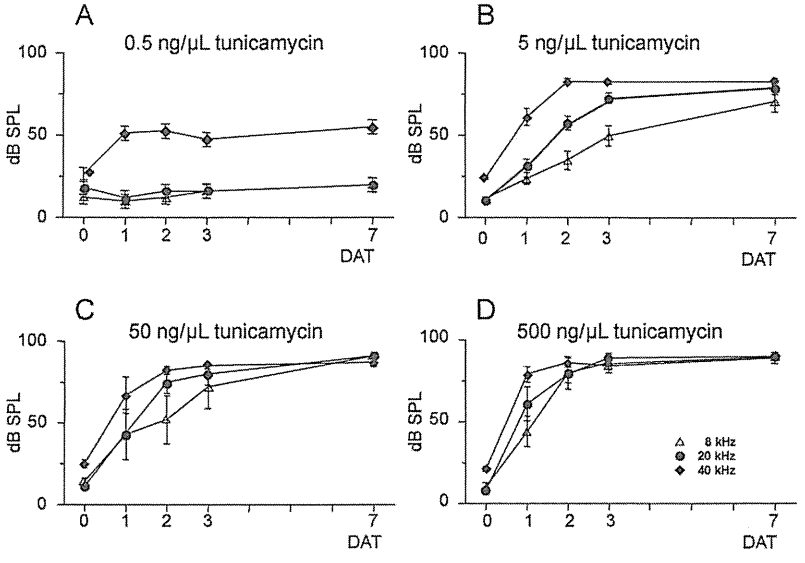

Fig. 1. Hearing loss following treatment with tunicamycin. A – D) ABR thresholds after treatment with different dosages of tunicamycin were measured at 8 kHz (open triangles), 20 kHz (closed circles), and 40 kHz (closed diamonds) for 7 DAT. 0 DAT: pretreatment. Data are shown as averages ± S.E.M.

DAT (Fig. 1A). The hearing level remained stable up to 7 DAT. The hearing levels at 8 and 20 kHz were not affected by this tunicamycin concentration. Treatment with 5 ng/μL tunicamycin induced ABR threshold shifts at all frequencies as early as 1 DAT. The thresholds developed to 66.6 ± 7.4 dB at 8 kHz, to 77.7 ± 5.5 dB at 20 kHz, and 82.7 ± 2.9 dB at 40 kHz 7 DAT (Fig. 1B). Increasing the tunicamycin dose to 50 ng/μL resulted in no ABR response to the maximum output of the system at all three frequencies measured 7 DAT, indicating that the rats lost hearing completely (Fig. 1C). With 500 ng/μL tunicamycin, the rats lost hearing completely at all three frequencies at 3 DAT (Fig. 1D). A mild temporary threshold shift at 40 kHz was observed in vehicle-treated animals at 3 DAT, but not in untreated animals, indicating an effect of surgical manipulation (data not shown).

Because the differences in ABR threshold shifts among the various tunicamycin concentrations were most prominent at 8 kHz, morphological changes in the middle turn of the cochlea, which is known to respond to approximately 5 to 15 kHz of sound (17), were observed 7 DAT (Fig. 2: A – J). Animals treated with 0.5 ng/μL tunicamycin showed the organ of Corti (OC) with a single row of inner hair cells (IHCs) and three rows of outer hair cells (OHCs) supported by Deiter's cells (Fig. 2: A, C), comparable to the vehicle-treated animals (Fig. 2: I, J), indicating no apparent degeneration. This is in agreement with normal hearing thresholds at 8 and 20 kHz following this tunicamycin dose (Fig. 1A). Treatment with 5 ng/μL tunicamycin (Fig. 2: B, D) induced the loss of OHCs in the OC (Fig. 2D), whereas the morphology of other cochlear tissues remained normal. With 50 ng/μL tunicamycin (Fig. 2: E, G), loss of LW fibrocytes (Fig. 2E, arrow) and the OHCs (Fig. 2G, asterisks) were evident. With 500 ng/μL tunicamycin, most of the spiral ganglion cells (SGCs) were lost (Fig. 2F, arrowhead). In addition, degeneration of the LW fibrocytes was severe compared with rats treated with 50 ng/μL tunicamycin, and degeneration of the Deiter's cells in addition to the HCs in the OC was observed (Fig. 2: F, H). Visualization of actin-rich stereocilia, critical structures in hair cells that transduce sound-induced mechanical vibrations, can be achieved by staining the cells with fluorescent dye-conjugated phalloidin. Gross degeneration of the OHCs by 5 ng/μL tunicamycin was confirmed by significant loss of stereocilia in the entire auditory epithelia (Fig. 2I). Vehicle treatment did not affect the stereocilia, which consist of three rows of OHCs and one row IHCs (Fig. 2L).

Ultrastructural changes of IHC synapses and SGCs

The frequent loss of OHCs in serial sections as observed by light microscopy was the most obvious pathological feature of hearing loss in animals treated with 5 ng/μL tunicamycin. OHCs are known to amplify sound sensitivities for roughly 50 – 60 dB (18). We set to ascertain whether loss of the OHCs alone account for the approximately 55 – 65 dB threshold shift at 7 DAT (Fig. 1B) by electron microscopic analysis of the IHCs and the SGCs in these animals.

Animals treated with 5 ng/μL tunicamycin showed normal morphology of the nucleus of the IHCs 7 DAT (Fig. 3A). However, the number of ERs appeared to be decreased compared with the IHCs in vehicle-treated animals (Fig. 3: B, E). In the synaptic region of the IHCs, vacuolar changes (Fig. 3C, open triangles) and multiple electron-dense granules (Fig. 3C, small arrows) were observed, indicating degeneration of the nerve endings. IHCs from animals treated with vehicle (Fig. 3: D – F) showed numerous subcellular organelles in the cytoplasm including mitochondria and ERs (Fig. 3: D, E, mt and asterisks). In the synaptic region of the IHCs, there appeared to be multiple nerve endings that descended from the SGCs (Fig. 3: D, F). Some of the nerve endings proximal to the IHCs formed electron-dense membranes, one of the features of postsynaptic membranes (19) (Fig. 3F, closed arrowheads). In tunicamycin-treated animals, numerous vacuoles and swollen mitochondria were observed in the cell bodies of SGCs 7 DAT, indicating degeneration of the SGCs (Fig. 3: G, H). In vehicle-treated animals, the SGCs contained multiple organelles including mitochondria and ERs without evidence of degeneration (Fig. 3: I, J).

Long-term effect of mild ER stress in the cochlea and early expression of ER stress marker genes

To study the long-term effects of tunicamycin-induced mild ER stress in the cochlea, rats treated with 5 ng/μL tunicamycin, which induced subacute and gradually progressive hearing loss, were selected to examine the ABR threshold shifts and morphological changes of the cochlea for up to 4 weeks. The ABR thresholds at 8, 20, and 40 kHz gradually and significantly increased to almost reach or exceed the maximum output 7 DAT (8 kHz), 3 DAT (20 kHz), and 2 DAT (40 kHz), respectively, and remained at this level up to 28 DAT (Fig. 4: A – C). The ABR threshold at 40 kHz increased more acutely than other frequencies of sound, the feature consistent with the primary experiment (Fig. 1B). The ABR threshold shifts in vehicle-treated animals did not show any significant difference between untreated animals in any frequencies of sound during experiment (Fig. 4: A – C).

ER stress is characterized by upregulation of several marker genes such as *chop*, *Atf4*, *grp78*, and *grp94*. To study early expression of ER stress markers in the co-

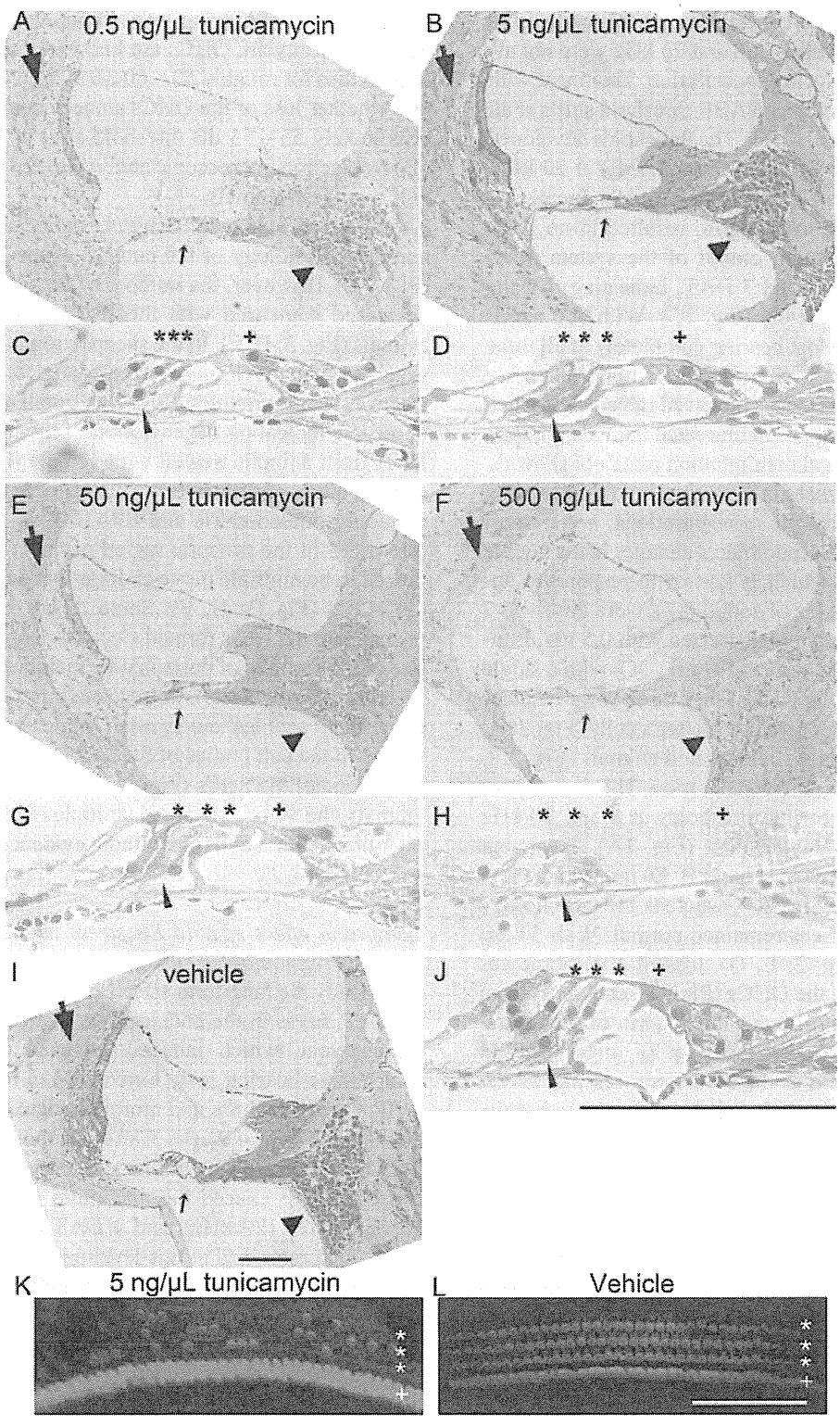

Fig. 2. Dose-dependent cochlear damage by tunicamycin. A, B, E, F, I) Morphology of the middle turn of the cochlea treated with various doses of tunicamycin or vehicle at 7 DAT. Magnified images of the organ of Corti are shown in panels C, D, G, H, and J. K, L) Surface preparations of organ of Corti in the corresponding turn with stereocilia visualized with rhodamine-phalloidin 7 DAT. Asterisks and plus indicate positions of OHCs and IHCs, respectively. Arrows, small arrows, arrowheads, and small arrowheads indicate LW, OC, SG, and Deiter's cells, respectively. Scale bar = 100 μm.

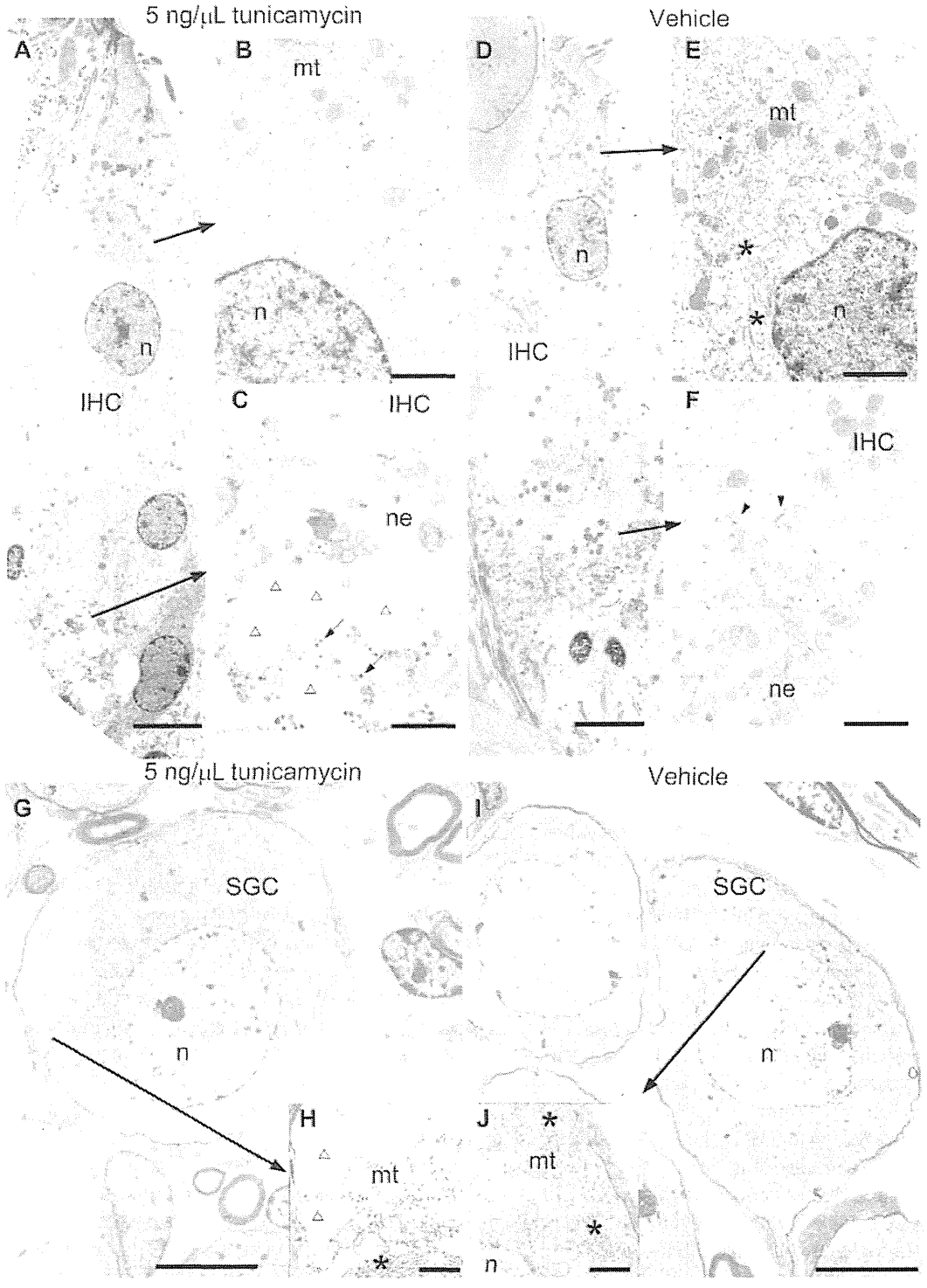

Fig. 3. Subcellular damage of IHCs and SGCs by tunicamycin. Electron microscopic images of IHCs (A – F) and SGCs (G – J) following treatment with 5 ng/μL tunicamycin (A – C, G, H) or vehicle (D – F, I, J) at 7 DAT. Panels B, C, E, and F are magnified images of the supranuclear or synaptic region of the IHCs, and panels H and J are the perinuclear region of the SGCs (arrows). In panels C and H, electron-dense granules and vacuoles caused by tunicamycin are indicated by small arrows and open triangles. In panels E and J, endoplasmic reticulum is indicated by asterisks. In panel F, electron-dense synapse membrane–like structures are indicated by closed arrowheads. IHC, inner hair cell; mt, mitochondrion; n, nucleus; ne, nerve ending; SGC, spiral ganglion cell. Scale bars in panels A, D, G, and I = 5 μm; scale bars in panels B, C, E, F, H, and J = 1 μm.

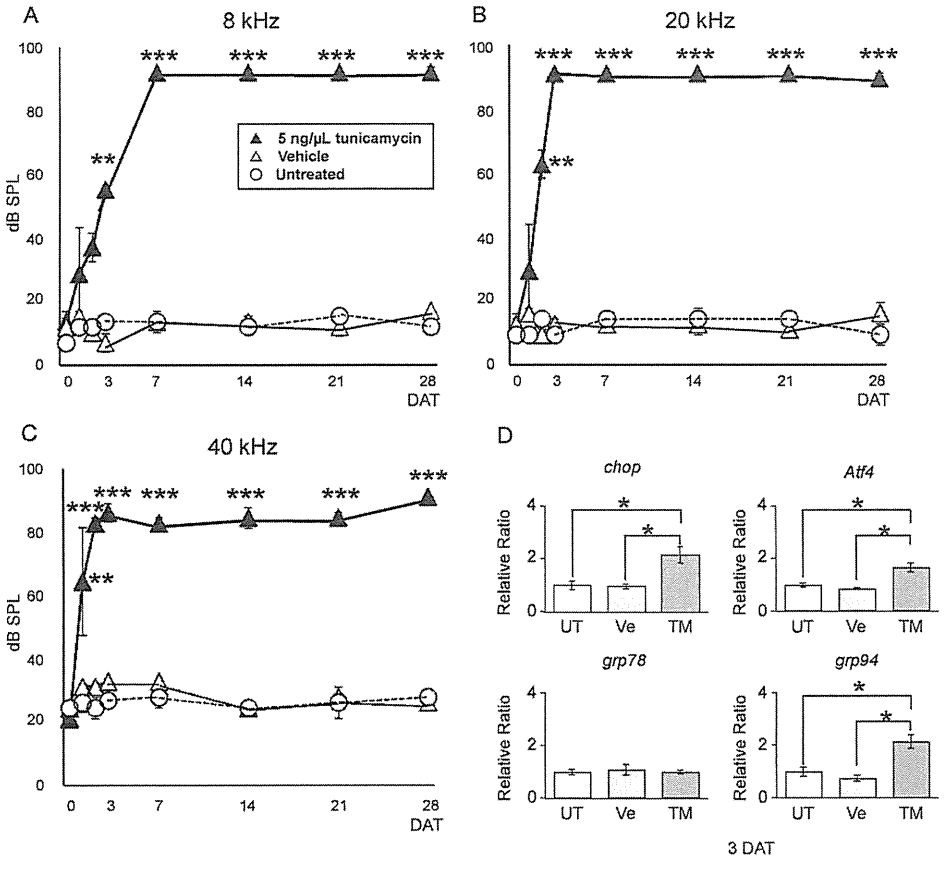

Fig. 4. Expression of ER stress response genes in the cochlea treated with 5 ng/μL tunicamycin. A – C) The ABR threshold in animals treated with either 5 ng/μL tunicamycin (closed triangles) or vehicle (open triangles) and that in untreated animals (open circles) were periodically measured until 28 DAT. Asterisks indicate significant differences between tunicamycin- and vehicle-treated animals. $^{**}P < 0.01$, $^{***}P < 0.001$, two-way ANOVA, n = 3. D) Expression of ER stress response genes in the whole cochlea 3 DAT. $^{*}P < 0.05$, Student's *t*-test with Holm's procedure, n = 3. UT, untreated; Ve, vehicle-treated; TM, treated with 5 ng/μL tunicamycin.

chlea, expression of these marker genes was evaluated with qRT-PCR in the whole cochlea (including LW, modiolus, OC, and surrounding connective tissues) from untreated animals, animals treated with vehicle, or those treated with 5 ng/μL tunicamycin at 3 DAT (Fig. 4D). As expected, expression levels of *chop*, *Atf4*, and *grp94* were significantly increased by tunicamycin treatment compared with vehicle-treated or untreated rats, confirming the tunicamycin-mediated ER stress in the cochlea. However, expression of *grp78* did not change significantly.

At 28 DAT, in addition to OHCs, the IHCs and Deiter's cells were severely degraded (Fig. 5: A, C) in tunicamycin-treated animals, whereas no significant morphological changes were evident in the LW and SGCs (Fig. 5A). The SGCs, LW, together with OHCs, IHCs, and Deiter's cells in vehicle-treated animals did not show morphological changes at 28 DAT (Fig. 5: B, D). Time-dependent, cell-specific morphological damage by tunicamycin is summarized in Table 1.

Disscussion

We established a novel animal model of subacute and gradually progressive hearing loss with perilymphatic perfusion of tunicamycin, which inhibits the first step of *N*-linked glycosylation in the ER (10), into the inner ear. Induction of ER stress marker genes in the cochlea and morphological changes after tunicamycin treatment indicated that the hearing loss was mediated by ER stress induced by tunicamycin.

We previously reported expression of ER stress marker genes in the cochlea in an animal model of acute cochlear mitochondrial dysfunction by mitochondrial toxin 3-NP (3). In the present model of subacute hearing loss by tunicamycin, a series of distinct features were identified, reflecting the different mechanisms involved in each model. Induction of *chop* in the cochleae by both acute mitochondrial dysfunction and acute ER stress indicates that the molecular pathways underlying the pathological process of the two types of hearing loss partially overlap. The mitochondrial vacuolation detected in SGCs in the tunicamycin-treated animals also appeared morphologically similar to the vacuolation observed in 3-NP-treated

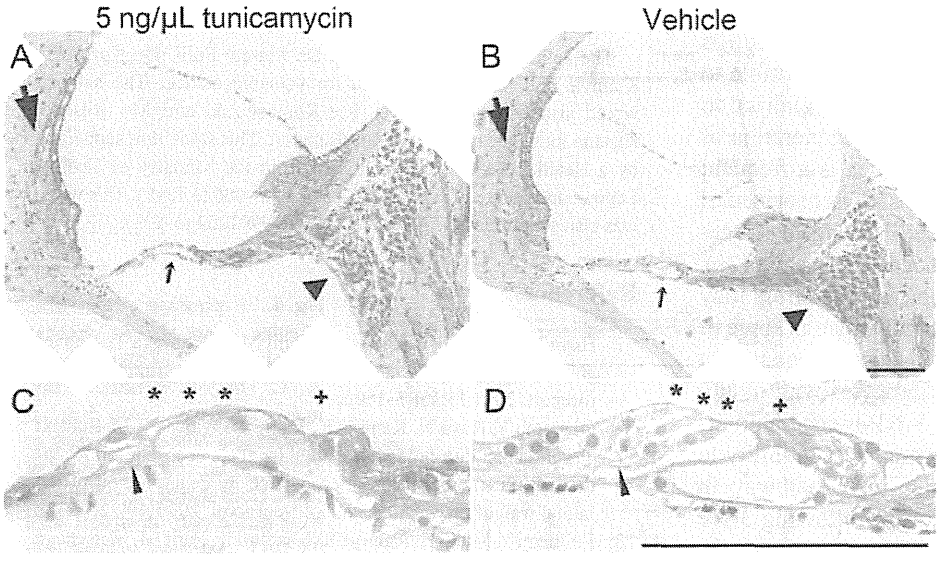

Fig. 5. Morphological damage of the OC by ER stress 28 DAT. Middle turn of the OC in animals treated with 5 ng/μL tunicamycin or vehicle is shown with paraffin sections and HE staining. The structure of the OC appeared markedly deteriorated in tunicamycin-treated animals (A, C) compared with the normal structure of the OC in vehicle-treated animals (B, D). As for symbols, please refer to Fig. 2. Scale bar = 100 μm.

Table 1. Morphological damage in the middle turn of cochlear cells by tunicamycin treatment

Treatment		7 DAT					28 DAT	
		Vehicle	0.5 ng/μL	5 ng/μL	50 ng/μL	500 ng/μL	Vehicle	5 ng/μL
Loss of	OHC	–	–	++	++	++	–	++
	IHC	–	–	–*	+	++	–	++
	Deiter's cell	–	–	–	–	++	–	++
	SGC	–	–	–*	+	++	–	–
	LW fibrocyte	–	–	–	+	++	–	–

–, no morphological damage; +, moderate loss of cells; ++, severe loss of cells; *, degeneration detected under electron microscopy.

animals (2). However, although SGCs in tunicamycin-treated animals demonstrated morphological changes 7 DAT, SGCs in 3-NP-treated animals showed a similar abnormality 3 h after treatment but returned to normal by 7 DAT (2). This difference is considered to reflect subacute and long-lasting effects of tunicamycin-induced ER stress (20) on SGCs and an acute and transient effect of 3-NP-induced mitochondrial dysfunction including ER stress on SGCs (3).

Hearing loss from tunicamycin progressed gradually and irreversibly even with the lowest dose of the drug, whereas low-dose treatment with 3-NP induces acute and transient hearing loss (1). The different time course of hearing loss between tunicamycin and 3-NP are not attributable to the distinct technical procedures between two animal models; tunicamycin was perfused into the perilymph through the semicircular canal to affect cochlear cells more directly and immediately than 3-NP, which was administered to the inner ear by permeation through the round window membrane (1). Progressive hearing loss by tunicamycin, however, occurred much more slowly than that by 3-NP. Onset of hearing loss by tunicamycin can be explained by inhibition of protein maturation in the ER of the cochlear cells that results in depletion of various functional molecules, depending on their turnover rates. The subsequent gradual progressive hearing loss by tunicamycin could be due to the time course of the entire molecular pathway of ER stress that is stimulated by tunicamycin and that leads to degeneration of cochlear cells (11). The irreversible increase in ABR thresholds with tunicamycin-induced hearing loss 28 DAT is consistent with loss of OHCs and loss of IHCs following degenerative changes of the subcellular organelles, both of which usually do not regenerate in mammals (21).

Histochemical study in tunicamycin-treated animals indicated that OHCs were the cell type in the cochlea most susceptible to the toxicity of ER stress. Because

hearing was primarily affected at high frequencies in tunicamycin-treated animals, OHCs in the basal portion of the cochlea are considered to be more susceptible to ER stress than those in the apical portion specialized to respond to lower frequencies of sound. Degeneration of OHCs in the basal portion of the cochlea is a frequent pathological feature in various types of sensorineural hearing loss, including drug-induced hearing loss, age-related hearing loss, and noise-induced hearing loss (22). It would be interesting to study whether ER stress may also be involved as a pathological mechanism in some of these types of sensorineural hearing loss. Predominant degenerative changes of the LW fibrocytes with induction of ER stress marker genes in 3-NP-treated animals (3) may be attributed to the differential susceptibility to mitochondrial dysfunction, a major toxic pathway in cochlear cells, in addition to ER stress following 3-NP treatment.

Induced expression of ER stress markers such as *chop*, *Atf4*, and *grp94* in the cochleae treated with tunicamycin is a direct evidence for ER stress. Interestingly, *grp78*, another major ER stress marker gene (23), was not up-regulated in the cochleae of tunicamycin-treated animals or in those of 3-NP-treated animals (3). Thus, the response to ER stress in the cochlea may not involve *grp78*. The association of ER stress with auditory function has also been suggested in Wolfram syndrome involving high-frequency hearing loss (24, 25) or hereditary non-syndromic low-frequency hearing loss (26, 27), both of which are caused by *WFS1* mutations. *WFS1* encodes an ER protein, wolframin. An in vitro experiment has shown that wolframin controls ER stress response through degradation of ATF6α in the normal state, thereby suppressing the downstream ER stress marker genes such as *grp78* and *chop* (28). Dysfunction of wolframin could result in increased expression of the ER stress marker genes and apoptosis. Wolframin is expressed in OHCs, SGCs, and LW fibrocytes (ref. 29 and data not shown). It is of our future interest whether the animal model of ER stress–induced hearing loss established in this study is helpful for considering molecular mechanisms of hereditary hearing loss caused by *WFS1* mutations.

In summary, we studied the physiological, morphological, and molecular features of a newly established animal model of hearing loss caused by tunicamycin-induced ER stress. This model is useful for elucidating the mechanisms of some types of hearing disorders that involve ER stress, and it may lead to identification of drug targets to treat such types of hearing loss.

Acknowledgments

The authors would like to thank Dr. Masato Fujii, Dr. Kazusaku Kamiya, and Dr. Takeshi Iwata for valuable advice. The authors would also like to thank Ms. Rie Komatsuzaki and Ms. Ritsuko Kusano for their excellent technical support. This study was supported by a Health Science Research Grant from the Ministry of Health, Labor, and Welfare of Japan (H16-kankakuki-006 to T.M.). This work was also supported by JSPS KAKENHI (19791252 to Y.F.).

References

1 Hoya N, Okamoto Y, Kamiya K, Fujii M, Matsunaga T. A novel animal model of acute cochlear mitochondrial dysfunction. Neuroreport. 2004;15:1597–1600.
2 Okamoto Y, Hoya N, Kamiya K, Fujii M, Ogawa K, Matsunaga T. Permanent threshold shift caused by acute cochlear mitochondrial dysfunction is primarily mediated by degeneration of the lateral wall of the cochlea. Audiol Neurootol. 2005;10:220–233.
3 Fujinami Y, Mutai H, Kamiya K, Mizutari K, Fujii M, Matsunaga T. Enhanced expression of C/EBP homologous protein (CHOP) precedes degeneration of fibrocytes in the lateral wall after acute cochlear mitochondrial dysfunction induced by 3-nitropropionic acid. Neurochem Int. 2009;56:487–494.
4 Katayama T, Imaizumi K, Manabe T, Hitomi J, Kudo T, Tohyama M. Induction of neuronal death by ER stress in Alzheimer's disease. J Chem Neuroanat. 2004;28:67–78.
5 Holtz WA, O'Malley KL. Parkinsonian mimetics induce aspects of unfolded protein response in death of dopaminergic neurons. J Biol Chem. 2003;278:19367–19377.
6 Tajiri S, Oyadomari S, Yano S, Morioka M, Gotoh T, Hamada JI, et al. Ischemia-induced neuronal cell death is mediated by the endoplasmic reticulum stress pathway involving CHOP. Cell Death Differ. 2004;11:403–415.
7 Araki E, Oyadomari S, Mori M. Impact of endoplasmic reticulum stress pathway on pancreatic beta-cells and diabetes mellitus. Exp Biol Med (Maywood). 2003;228:1213–1217.
8 Sato S, Ward CL, Krouse ME, Wine JJ, Kopito RR. Glycerol reverses the misfolding phenotype of the most common cystic fibrosis mutation. J Biol Chem. 1996;271:635–638.
9 Xu C, Bailly-Maitre B, Reed JC. Endoplasmic reticulum stress: cell life and death decisions. J Clin Invest. 2005;115:2656–2664.
10 Elbein AD. Inhibitors of the biosynthesis and processing of N-linked oligosaccharides. CRC Crit Rev Biochem. 1984;16:21–49.
11 Takatsuki A, Arima K, Tamura G. Tunicamycin, a new antibiotic. I. Isolation and characterization of tunicamycin. J Antibiot (Tokyo). 1971;24:215–223.
12 Oyadomari S, Mori M. Roles of CHOP/GADD153 in endoplasmic reticulum stress. Cell Death Differ. 2004;11:381–389.
13 Inokuchi Y, Nakajima Y, Shimazawa M, Kurita T, Kubo M, Saito A, et al. Effect of an inducer of BiP, a molecular chaperone, on endoplasmic reticulum (ER) stress-induced retinal cell death. Invest Ophthalmol Vis Sci. 2009;50:334–344.
14 Siliprandi R, Canella R, Carmignoto G, Schiavo N, Zanellato A, Zanoni R, et al. N-methyl-D-aspartate-induced neurotoxicity in the adult rat retina. Vis Neurosci. 1992;8:567–573.
15 Konno T, Watanabe J, Ishihara K. Enhanced solubility of paclitaxel using water-soluble and biocompatible 2-methacryloyloxy-